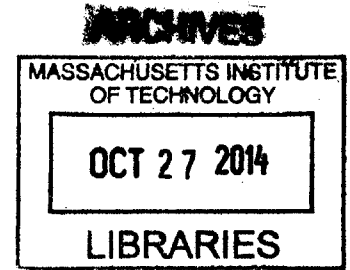# Experiments in Fluid Spreading
in the Partial Wetting Regime

by

Michael A. Chen

S.B. Environmental Engineering
Massachusetts Institute of Technology, 2012

Submitted to the Department of Civil and Environmental Engieering
in partial fulfillment of the requirements for the degree of

Master of Science in Civil and Environmental Engineering

at the

MASSACHUSETTS INSTITUTE OF TECHNOLOGY

September 2014

Signature redacted

Signature of Author:. . . . .
Department of Civil and Environmental Engieering
August 13, 2014

Signature redacted

Certified by:. . . . .
Ruben Juanes
Associate Professor of Civil and Environmental Engineering
Thesis Supervisor

Signature redacted

Accepted by:. . . . .
Heidi M. Nepf
Donald and Martha Harleman Professor of Civil and Environmental
Engineering
Chair, Department Committee on Graduate Theses

Experiments in Fluid Spreading

in the Partial Wetting Regime

by

Michael A. Chen

Abstract

The spread of a fluid on a flat surface has been the subject of intense research for a number of decades, having importance in surface treatment technologies, porous media flow, and common naturally ocurring phenomena. In the complete wetting case, a fluid will spread until it can cover the entire surface with a thin film of molecular thickness; the dynamics of these fluids are well understood. In the partial wetting case, the fluid first spreads and then stops, forming a puddle. Research on partial wetting flows has revealed that the macroscopic behavior is impacted by microscopic behavior, but there is no broadly accepted model that connects these two regions. Some experimental data exist for a small volume of partial wetting fluid spreading, but there is a distinct gap in data for larger volumes.

Here, we first review currently established understanding of the spreading problem for the complete wetting and partial wetting cases. We then present the results of laboratory experiments for large volume fluid spreading in the partial wetting regime. We observe an early time spreading regime, which is followed by a relaxation to steady state. Comparisons to similarly large volumes of a complete wetting fluid spreading show differences even in the early time behavior. We compare the results of these experiments with a macroscopic model in development and find agreement between experiment and model, with the model revealing an early spreading regime of the form $A \sim t^{\frac{1}{4}}$. The results of these experiments and model of simple fluid spreading lay the foundation for future work investigating more complex multiphase flow phenomena in porous media under the partial wetting regime.

Thesis Supervisor: Ruben Juanes
Title: Associate Professor of Civil and Environmental Engineering

Acknowledgments

I am blessed to be surrounded by an amazing, supportive group of friends, family, and colleagues, without whom, I would not have been able to complete this thesis. In particular, I would like to thank:

My thesis advisor, Ruben Juanes, for his clear guidance and advice;

Professor John Bush and his student Dan Harris for their invaluble help and use of their lab as I designed the experimental set up;

Pietro De Anna, Mathias Trojer, and Amir Pahlavan for their innovative suggestions on how to improve all aspects of these experiments and patient assistance as I built an understanding of the theory of the spreading problem;

My parents Reginald and Katherine Chen, and my sister Christine Chen, for their limitless love and support.

Contents

List of Figures

Chapter 1

Introduction: Thin Film Flows and Fluid Spreading

The flow of a thin film of fluid is a common phenomenon in everyday life. From the protective coating on the cornea of the eye, to rainwater sliding down a window pane or a spilt drink, we interact with thin films on a regular basis. In spite of their ubiquity, they contain within a plethora of fascinating behavior which has been the subject of study for many years. One notable problem is the spread of a fluid on a flat surface, which, contrary to its conceptual simplicity, remains challenging to predict in some scenarios. Thin film flows represent a fundamental multiphase flow problem, and developments in understanding of this simple problem may be able to assist the solution of more complicated problems such as multiphase flow in porous media.

1.1 Thin Film Flows

Thin film flows have been the subject of focused study for many years, and are a commonly occurring phenomenon seen in unsaturated porous media flow [16], printing, and coatings used to protect or modify surfaces. There has been a significant amount of work done to probe the dynamics of these flows [18], but many important questions remain unanswered. The equations describing such flows are nonlinear, and modeling thin flim behavior provides a continued source of academic discourse [6].

Flow on heterogeneous surfaces [12] and the role thin films play in dynamic systems such as splashing drops [14] are other notable problems relating to thin films.

Deeply intertwined in probing thin films is the study of surface wettability, which has recently experienced increased public interest with the development of super oleophobic surfaces [24] and commercial products boasting super hydrophobic properties. The design of these surfaces is of importance to the maintenance and protection of surfaces in a variety of conditions. The wettability of a surface also plays an important role in the dynamics of two fluids near a solid surface. In a complete wetting case, the wetting fluid tends toward covering the surface entirely, while in the partial wetting case, the wetting fluid experiences a constrained flow. There already exists a large body of work reviewing the details of complete wetting flows [2], but there is much left to study in partial wetting systems. One representative problem where this discrepancy in understanding is apparent is the dynamics of a spreading fluid on a solid surface.

1.2   Liquid Spreading

How a fluid spreads in air on a flat, level, solid surface is a classic problem that has been studied for many decades. Early work examined the static configuration of a drop of fluid, finding a force balance between the three phases given by Young's equation [25],

$$\gamma_{SV} = \gamma_{SL} + \gamma \cos(\theta_{eq}) \tag{1.1}$$

where γ_{SV} represents the solid-vapor surface tension, γ_{SL} the solid-liquid surface tension, γ the liquid vapor surface tension, and θ_{eq} the equilibrium contact angle. Figure 1-1 gives a schematic of these surface tensions acting as line forces at the intersection of the three phases. This interface is named the contact line. Note that θ_{eq} is *macroscopically* defined, and does not account for forces or behavior at the microscopic scale [7].

Reinterpreting the line forces in 1.1 as surface energies, it is then possible to define a spreading parameter, S_{eq}, to describe the wetting state of a system at thermody-
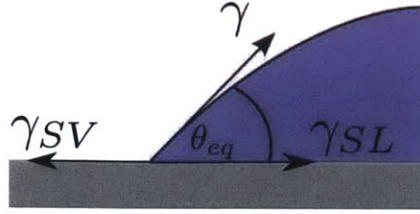
Figure 1-1: Schematic of a partial wetting static drop in some passive gas with surface tension force balance at the contact line.

namic equilibrium,

$$S_{eq} = \gamma_{SV} - (\gamma_{SL} + \gamma) = \gamma \left(\cos \theta_{eq} - 1 \right) \tag{1.2}$$

For $S_{eq} \geq 0$, the energy of the dry surface is balanced by the combined energy of the wet surface and air liquid interface, resulting in a film of fluid that covers the entire surface to minimize the system energy. This is called complete wetting. For $S_{eq} < 0$ and $0° \leq \theta_{eq} \leq 90°$, the energy of the system is minimized by the formation of a finite fluid area, with a dry portion remaining, which is called partial wetting. Larger contact angles with $S_{eq} < 0$ are termed non-wetting systems. A feature of the partial wetting system at *thermodynamic* equilibrium is that there are adsorbed molecules of the fluid attached to the soild surface throughout [2]. Figure 1-2 displays a schematic of these different wetting states. γ_{SV} is not a measurable quantity [20], and the spreading parameter prescribes only the equilibrium contact angle. As a result, the details of the shape of a fluid mass are not part of this description. In practice, thermodynamic equilibrium can be difficult to achieve, and it is more common to observe fluids that are in a static configuration, but are not necessarily at thermodynamic equilibrium.

It is also possible to define an initial spreading parameter, S_i, for a droplet spreading out of thermodynamic equilibrium, where γ_{SO} replaces γ_{SV} in equation 1.1. γ_{SO} represents the energy of surface far from thermodynamic equilibrium without adsorbed fluid molecules [7]. Positive values of S_i favor the spread of a liquid as one might expect, though there is no longer a clear relation with θ_{eq}. The dynamics of

(a) Equilibrium state for a complete wetting fluid   (b) Equilibrium state for a partial wetting fluid with contact angle θ_{eq}.
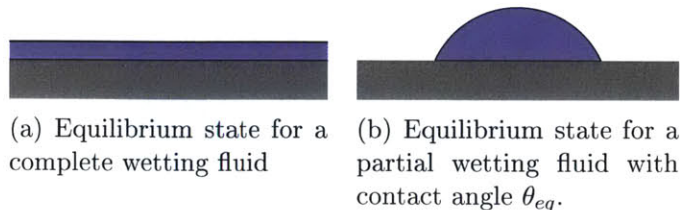
Figure 1-2: Schematic of a fluid at equilibrium in various wetting states.

the spreading fluid are not described by the spreading parameter.

The dynamics of a spreading fluid have also been of interest for the past few decades. A variety of scaling laws, describing the evolution of a drop or small mass of fluid, were developed through some experiments [23, 13], and take the form of $R \sim t^n$, where R is the fluid's radial extent, t is the time elapsed, and n is some exponent relating to the regime of flow. These power laws were then confirmed by further experimental work for small drops in the complete wetting state [21, 4]. Of note are experiments with well controlled thermal conditions, which also confirm these scalings [10], as well as experiments with larger volumes of fluid [21, 17]. A more in-depth treatment of the mathematics of these dynamics is given in Chapter 2. Despite some difficulties, particularly in resolving the motion of the contact line, complete wetting spread is well characterized at a variety of scales. Current research focuses on the dynamics on surfaces with defects, as well as the dynamics of partial wetting systems, where contact line motion is not clearly understood [2].

1.3   Motivation

With a few exceptions, the study of these spreading fluids has been mainly restricted to small droplets in the complete wetting state. There is very little experimental work examining the spread of large volumes of fluid in a partially wetting system. Studies of thermal impacts on spreading included a few experiments with drops in a partial wetting system [10], and a few others captured the spread of a droplet, and fit its exponential relaxation [15]. Common sense along with understanding of the spreading parameter predicts that a mass of fluid in a partial wetting system will have a finite

area at equilibrium. To date, however, there is little, if any, data on the partial wetting spread of volumes of fluid larger than 10 mL. We seek to contribute experimental data in hopes of providing useful comparison with theoretical descriptions and simulations of similarly large volumes of fluid in partial wetting systems.

Chapter 2

Overview of Thin Film Mathematical Modeling

There is a significant amount of research devoted specifically to the mathematical and theoretical treatment of thin films flows. Here, we will give a cursory overview of this research, with a focus on the problem of spreading. For a more in-depth review, the reader is directed toward the references [2], [5], and [8]. First we will cover complete wetting, followed by partial wetting, and we will end with a discussion of open questions in the mathematical description of thin films.

2.1 Complete Wetting

The spread of a complete wetting fluid mass on a level, flat, solid surface, in a passive gas is governed by the thin film equation. A sketch of the problem is shown in figure 2-1. The equation is derived from the Navier-Stokes equation using the lubrication approximation [18]:

$$\mu \frac{\partial h}{\partial t} + \nabla \cdot \left[-\frac{1}{3}\rho g h^3 \left(\nabla h - \frac{\gamma}{\rho g} \nabla \left(\nabla^2 h \right) \right) \right] = 0 \tag{2.1}$$

The small height, h, and large horizontal extent of a spreading fluid justify the use of the lubrication approximation. This formulation shows that either gravity
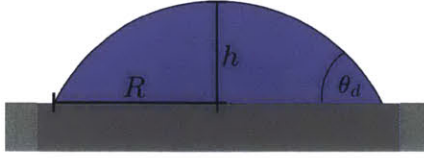
Figure 2-1: Diagram of a spreading mass of non-volatile fluid on a flat surface of density ρ, viscosity μ, and volume V_o. Note the dynamic contact angle, θ_d, is not the equilibrium contact angle, θ_{eq}.

or capillarity can drive flow, and that viscosity dissipates the work done by these forces. From this equation, it is relatively simple to construct some simple scalings for the evolution of the radius of an axisymmetric, complete wetting drop spreading over time. The volume of the drop is given as $V_o \approx R^2 h$ for a drop of radius, R, and height, h. For the case where gravity is negligible, we can define a capillary force which scales as $\gamma \theta_d^2$, with a dynamic contact angle θ_d. This capillary force is compared to a viscous force $\mu U R / h$ where $U = \frac{dR}{dt}$, the velocity of the contact line. Solving for U, we find:

$$\frac{dR}{dt} \propto \frac{\gamma \theta_d^2 h}{\mu R} \tag{2.2}$$

Since $\theta_d \propto \tan \theta_d \propto h/R$ for sufficiently small angles, it is then possible to rewrite equation 2.2 in terms of the radius and height of the drop:

$$\frac{dR}{dt} \propto \frac{\gamma h^3}{\mu R^3} \tag{2.3}$$

Substituting the volume of the drop for the height, and integrating in time then gives:

$$R \propto t^{\frac{1}{10}}, \quad A \propto t^{\frac{1}{5}} \tag{2.4}$$

This derived scaling corresponds to Tanner's law [23], which is reported for the spread of a complete wetting fluid in which gravity forces are negligible. The easiest way to define this regime's occurrence is through the capillary length, κ^{-1}:

$$\kappa^{-1} = \sqrt{\frac{\gamma}{\rho g}} \tag{2.5}$$

For $R \ll \kappa^{-1}$, gravity is negligible, and the scaling derived applies in the case of a spreading droplet. When this condition is not met, the force of gravity becomes signficant and an alternate scaling can be derived. Instead of capillary force, we compare the gravitational force $\rho g h^2$ to the viscous force. In a similar manner as above, we then find:

$$R \propto t^{\frac{1}{8}}, \quad A \propto t^{\frac{1}{4}} \tag{2.6}$$

This spreading regime as well as Tanner's law has been observed experimentally for complete wetting droplets spreading on a variety of surfaces [4]. These relations allow for the verification of numerical techniques used to solve the thin film equation for a drop spreading [11].

A complication arises in this hydrodynamic solution at scales smaller than the macroscopic scale, deriving from the initial definition of the contact angle in equation 1.1. Microscopic behavior is not prescribed in this problem formulation, and common constructions of Navier-Stokes prescribe a no-slip boundary condition at the solid-liquid interface. The movement of the contact line is at odds with this condition, and a singularity in the fluid stress results. This is called the moving contact line problem, which has been a leading problem in thin film dynamics. The problem creates a challenge in formulating the boundary conditions for a spreading fluid mass [9]. The advent of highly accurate ellipsometry, as well as advanced surface treatment techniques, has allowed scientists to probe the regions near the contact line, and uncover the presence of a microscopic precursor film [20]. Thus, the moving contact line problem is circumvented, as the bulk fluid flows on a preceding film of itself. The situation changes for a partial wetting fluid, which will be examined in the next section.
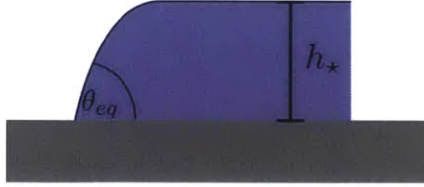
19

Figure 2-2: Schematic of a spreading fluid where the influence of gravity is felt, resulting in a pancake shape.

2.2 Partial Wetting

Solving equation 2.1 for a partial wetting system gives incorrect results, namely, the solution does not predict the halt of fluid spreading. Theory predicts that the radius of a fluid mass controls its final shape in an axisymmetric system [8]. In the regime where $R \ll \kappa^{-1}$, the fluid takes the form of a spherical cap due to the dominant capillary forces, intersecting the solid surface at θ_{eq}. For $R \gg \kappa^{-1}$, however, the fluid mass takes on a pancake like shape with height $h_\star$ given by [8]:

$$h_\star = 2\kappa^{-1} \sin\left(\frac{\theta_{eq}}{2}\right) \tag{2.7}$$

This height results from the force balance of capillarity given by Young's law and hydrostatic pressure. The edges of the fluid intersect with the surface at θ_{eq}, and rise up to the fluid thickness given by $h_\star$ in figure 2-2. The traditional thin film equation does not predict this final configuration, or that of a small partial wetting drop, thus the scalings derived in section 2.1 are not necessarily applicable for this flow. Despite these inaccuracies in equation 2.1, it is possible to use this equation to derive a non-dimensional time to scale data with. We choose to pick a time scale that marks when the effects of gravity cease to act on the puddle. First we rewrite the equation in radial coordinates, neglecting the capillarity term:

$$\frac{\partial h}{\partial t} - \frac{\rho g}{3\mu r} \frac{\partial}{\partial r}\left(r h^3 \frac{\partial h}{\partial r}\right) = 0 \tag{2.8}$$

This form corresponds with forms previously reported for an axisymmetrically spreading drop [13]. We use the equilibrium state to pick the following characteristic

length scales: for the height, we pick $h_\star$, and for the radius, r, we pick the equilibrium radius $R_\star = \sqrt{V_o/h_\star}$. To complete the non-dimensionalization, we can then define the characteristic time, t_c as:

$$t_c = \frac{3\mu R_\star^2}{\rho g h_\star^3} \tag{2.9}$$

To nondimensionalize the areas, we simply pick the final area:

$$A_\star = V_o/h_\star \tag{2.10}$$

When comparing to historical complete wetting data, we will use the same characteristic area and time, even though for a complete wetting fluid, $h_\star$ is meant to be zero. We expect, based on this scaling, that for experiments displaying the same contact angle θ, the curves describing the areal evolution over time will collapse.

Preceeding this work are a number of experiments examining the spread of partially wetting drops. Studies of the early time spreading as a drop just impacted a surface suggested an inertially dominated regime where the area evolves in an equation of the form $A \sim t^n$, where n depends on the equilibrium contact angle [1]. Other work examined the transition to steady state, proposing an exponential power law relaxation [15]. The presence of a dynamically varying contact angle, which does not match the equilibrium contact angle, complicates prediction and characterization of partial wetting flows in all time regimes. The time dependent contact angle is tied to questions of fluid behavior at the contact line, which remain unanswered for partial wetting systems [2]. It is clear that microscopic features have some notable impact on the macroscopic spread, but there is not a currently established method to reliably connect the flow at these two scales.

2.3   Open Questions in the Problem of Spreading

As noted previously, there remain a number of open questions in the mathematics of fluid spreading. A key question revolves around the moving contact line problem,

where formulating boundary conditions for solving thin film flow problems remains uncertain [22]. There are many proposed theories about the physical behavior at the contact line, and there are equally many numerical techniques used to circumvent or resolve the contact line singularity [2]. These uncertainties are generally connected with the development of a complete formulation for the spread of a fluid droplet, and clearly indicate a need for a theory connecting macroscopic flow in the bulk of a fluid and microscopic/mesoscopic flow near the contact line. Improvements in experimental techniques can help reveal the physical phenomenon occurring.

A second open question is the derivation of a macroscopic model for a partial wetting fluid flow. One promising approach takes advantage of a Cahn-Hilliard framework, modeling the movement of the spreading fluid by tracking the system free energy E [3]. The free energy is composed of two components, the bulk free energy $f(h)$, and the interfacial energy, $\kappa(h)$. These are given by:

$$f(h) = \frac{1}{2}\rho g h^2 - S + E_1(h) \tag{2.11}$$

$$\kappa(h) = \gamma + E_2(h) \tag{2.12}$$

Note the terms E_i in both energy terms refer to a microscopic contributions to the free energy resulting from the microscopic features of the spreading fluid. The final form of the evolution equation is given by:

$$\frac{\partial h}{\partial t} = \frac{\partial}{\partial x}\left(h^3 \frac{\partial}{\partial x}\left(\frac{\partial f}{\partial h} - \mathrm{Bo}^{-1}\sqrt{\kappa(h)}\frac{\partial}{\partial x}\left(\sqrt{\kappa(h)}\frac{\partial h}{\partial x}\right)\right)\right) \tag{2.13}$$

A more detailed derivation of this particular model can be found in [19], and its results will be used to compare with the experimental results of this work. Given the correct microscopic energies E_i, it is possible to model the macroscopic fluid spread, without explicitly modeling the fluid behavior near the contact line region as well as determine the macroscopic contact angle and contact line speed U.

Chapter 3

Experimental Investigation

We have conducted a series of experiments allowing a large ($R \gg \kappa^{-1}$) mass of fluid to spread under gravity after being deposited onto a flat, level, partial wetting surface until the mass reaches a steady state. To characterize this spread, we image the fluid mass and calculate its area over time. We vary the volume of fluid in each experiment, while keeping constant the density, viscosity, and equilibrium contact angle. This set of experiments represents a useful initial data set of large volume partial wetting fluid spread.

3.1 Experimental Set Up

We choose a 1000 cSt Silicone Oil from Sigma Aldrich, dyed with Orcosolve Blue Oil dye at a concentration of $0.07\,\mathrm{g\,L^{-1}}$. The mass of fluid that is on the surface is measured for each experiment, and is then converted to volume with the manufacturer reported density of $0.971\,\mathrm{g\,mL^{-1}}$. For the experimental surface, we use a flat, 60 cm by 60 cm by 0.65 cm borosilicate glass which is treated manually with Nanogate Pro Glass Clear 105 surface treatment. The thickness tolerances, as reported by the distributor of the glass, are 0.02 cm. The advancing contact angle for this fluid, air, and this treated surface was measured with a goniometer and is $(75 \pm 3)°$. Before starting an experiment, the surface is cleaned with isopropyl alcohol, and treated with the pro glass compound. After an experiment, the surface is cleaned by mechanically
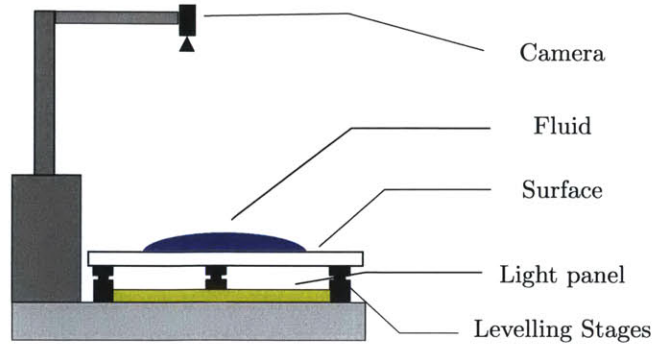
Figure 3-1: Schematic of experimental setup

removing the silicone oil, followed by cleaning with isopropyl alcohol. The same surface is used for subsequent experiments.

The glass surface is levelled with a Starret Machinist Level before each experiment to an accuracy of 1/2400. This is accomplished by the use of micrometer driven vertically translating stages attached to an optical table. In addition, the micrometer reading is taken after levelling the surface, and after the experiment, to establish that the levelness was maintained over the course of the experiment. The fluid is deposited from a beaker on to the glass while kept at a height close to the surface, without allowing the beaker to touch the surface. Once the fluid is deposited, the experiment is imaged from above until the mass reaches a static configuration. Typical experiment times were one to two days. A schematic of the experimental setup can be seen in figure 3-1.

To study the spread of a mass of fluid on a partial wetting surface, we choose to examine the evolution of the fluid area over time. The fluid mass is illuminated from below with a light panel, and imaged at 16 bit-depth from above using a Pike AVT firewire camera with a 16 mm focal length lens controlled with a MATLAB script. The camera is sufficiently far from the surface that the whole surface can be seen, but we do not explicitly measure the camera height. The script allows for the measurement of the time each picture is taken to accuracy of milliseconds.

To get an independent measure of the fluid height, we also took images of the fluid in its static condition from the side with a macro lens. We used a Canon EOS

1D DSLR, along with a 65 mm macro lens at 1x zoom. In this way, we were able to measure the height of the pancake of fluid, independent of the volume and area measurements. The height mesaured was (1.8 ± 0.1) mm. To compare, we calculate the height of the final fluid configuration by dividing the measured volume by the experimental area. This assumes the edges are insignificant in their contribution to the volume. Using this approach, we find a average height, h_*, of (1.7 ± 0.1) mm.

3.2 Image Processing

The raw experimental images, which are greyscale PNG files, are processed using a MATLAB script. A background image of the illumintaed surface is taken before each experiment, and is subtracted from the original image. Then, a region of larger than 100 by 100 pixels up to 200 by 200 pixels is selected such that it is always in the spreading fluid mass over the course of the experiment, and the average region intensity is found at each time step. A value of 50% of that average intensity in this region is used as the threshold value to convert the greyscale image into a binary image. The total area is found by then counting the number of black pixels in the image over both dimensions. Before each experiment is run, an image of a known measurement scale is taken, and used to establish the conversion from pixels to cm, giving the area of fluid in each image, with a known time. The measurement uncertainty in the area is $< 6\%$.

Some experiments showed variations in the area, even after appearing to reach a steady configuration, or, upon visual inspection, showed a clear preferential flow. Given that we expect the spread to be homogenous excepting for heterogeneities in the surface, we expect the spread to be relatively even in all directions. Since it was not clear these expeirments had reached a static configuration, we have excluded the results of those experiments in the subsequent analysis.

Chapter 4

Results and Analysis

The results of the experiment in chapter 3 are reported here, detailing the spread of a mass of partial wetting fluid on a flat glass surface. In addition to this data, we will also compare these results to some historical data for the complete wetting case [17]. The equilibrium height of the fluid was measured, and can also be calculated based on the area, giving insight into whether the fluid mass has reached equilibrium. Finally, we compare the results of these experiments with modeling results from [19], examining possible earlier spreading regimes.

4.1 Experimental Results

The results of the experiments in chapter 3 follow. The area of the fluid mass at a given time is scaled by A_c, and the time is scaled by t_c, as described in section 2.2. Figure 4-1 displays the evolution of the spreading area of the fluid masses over time. The volume of the spreading fluid does not appear to have significant importance in this scaling of the spreading, and we see that the equilibrium area matches reasonably well with the one predicted by theory. We suspect that deviations from the theoretical equilibrium area result from heterogeneities in the surface, which are apparent when examining the spread of the fluid, which was not perfectly circular. These heterogeneities could be either physical or chemical in nature. An image of a typical experiment at its end is shown in figure 4-2 for reference. We can then compare these data to the
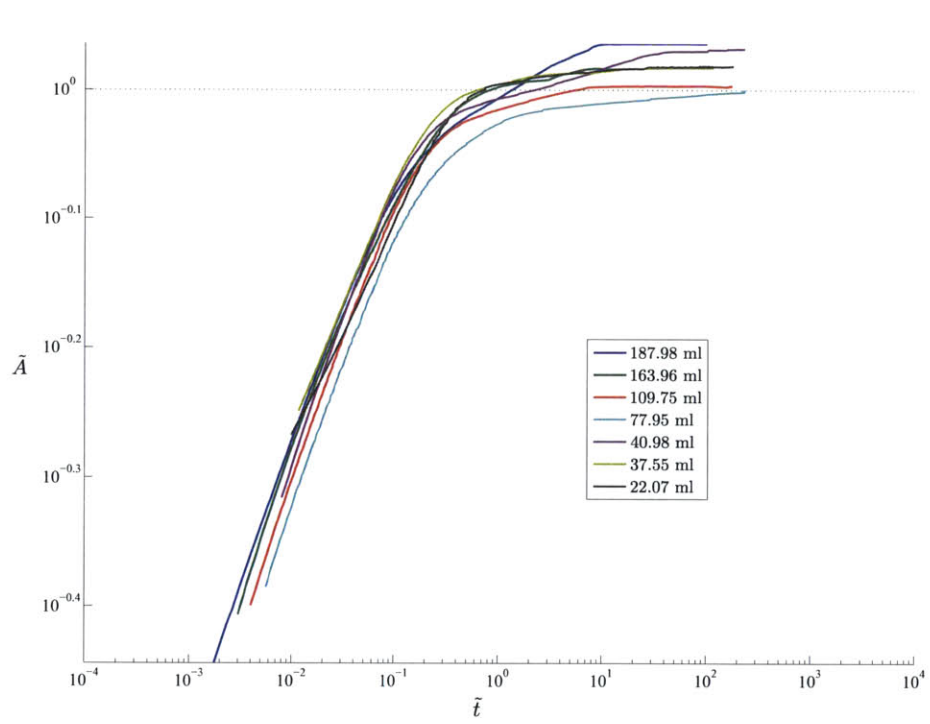
27

Figure 4-1: Time evolution of the spreading area for various volumes of silicone oil spreading on a flat, partial wetting surface. $\tilde{A}$ is the non-dimensional area, while $\tilde{t}$ is the non-dimensional time. The dotted line is placed at $\tilde{A} = 1$ for reference.
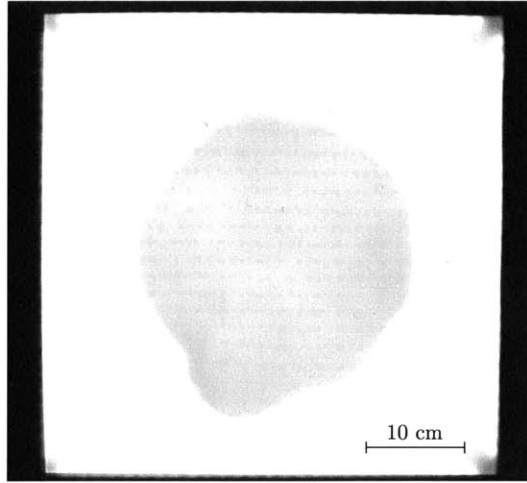
Figure 4-2: Image of the end of an experiment, with the mass of silicone oil in a static configuration. Heterogeneity in the surface can cause deformations in the circular shape of the fluid mass.

complete wetting data reported in figure 4-3 [17]. We scale the data using the same A_c and t_c, recognizing that for the complete wetting case, there will be no static equilibrium state where $\tilde{A} = 1$. Previous data on complete wetting spreading shows similar early time behavior. The late time behavior, however, as predicted by theory, is drastically different, with the complete wetting case showing no significant change in the spreading rate, while the partial wetting case exponentially relaxes to a static state.

For the given system described in chapter 3, we can calculate the expected pancake height based on equation 2.7, which gives $(1.8 \pm 0.1)\,\mathrm{mm}$. We can compare $h_\star$ with measurements of the fluid mass profile taken, which were $(1.8 \pm 0.1)\,\mathrm{mm}$ by imaging, and $(1.7 \pm 0.1)\,\mathrm{mm}$ based on the average area and measured volume. These measurements all closely agree with the expected value, suggesting the fluid masses had reached an equilibrium state at the experiment end.

4.2 Analysis and Comparison with Modeling Results

Examining these results suggests the possiblity of a spreading law of the form $A \sim t^n$. For complete wetting, we observe $A \sim t^{0.24}$, which is close to the behavior predicted in
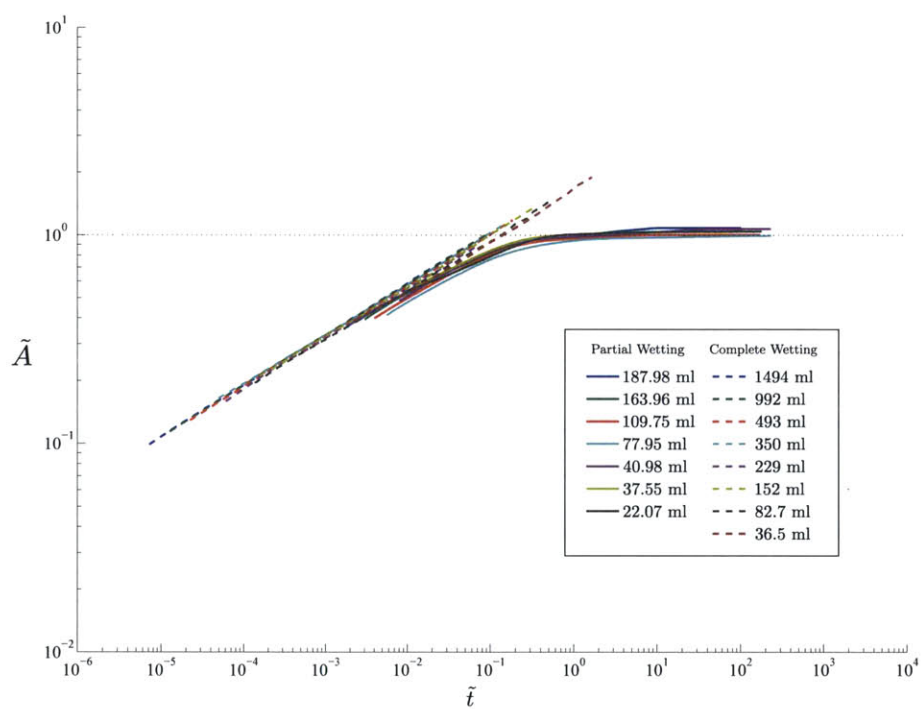
29

Figure 4-3: Comparison of partial wetting fluid spread data (solid lines) with complete wetting data from [17] (dashed lines). A dotted line is placed at $\tilde{A} = 1$ for reference.
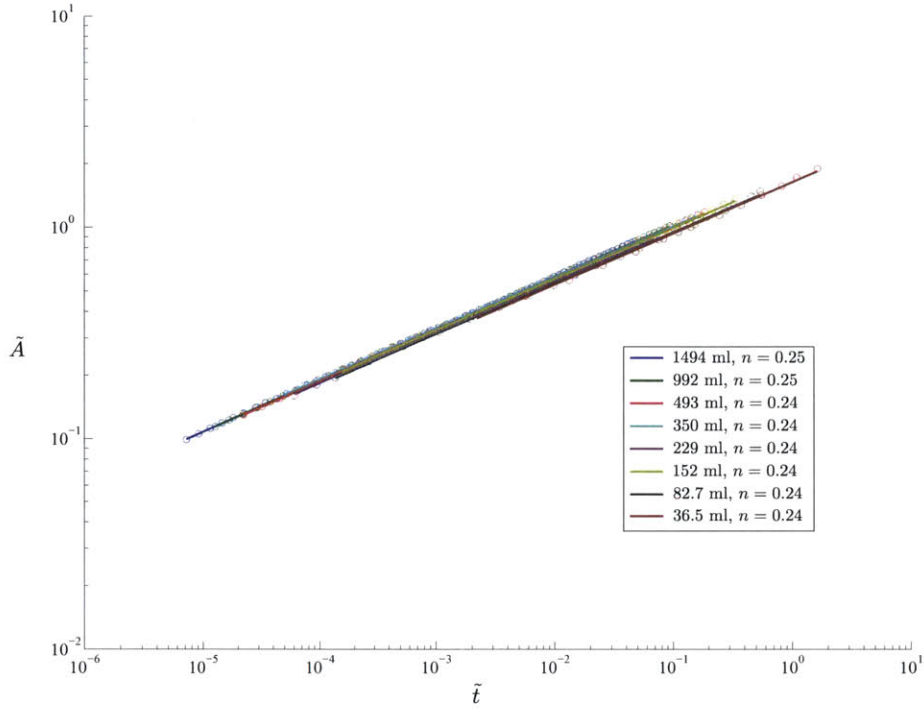
Figure 4-4: Nondimensionalized spread of various volumes of silicone oil in a complete wetting system, fitted with a power law relation of $\tilde{A} \sim \tilde{t}^n$. Lines represent the fit for a given volume, while ○ represent the actual experiment data gathered from [17].

equation 2.6 for spreading driven by gravity forces and balanced by viscous dissipation as we can see in figure 4-4. This behavior has been documented in a variety of sources, as discussed in chapter 2. For partial wetting systems, we see a possible power law matching the partial wetting behavior with $n = 0.20 \pm 0.02$ figure 4-5. This value of n does not have a clear corresponding theoretical derivation, with corresponding force balance, unlike in the complete wetting case. It is possible that the flow is driven by gravity, with the energy dissipation occurring both due to viscosity as well as behavior at the contact line. In order to build some insight into these partial wetting early time behaviors, we then compare the partial wetting behavior to the results of modeling .

We use equation 2.13 to model $7\,\mathrm{mL}$ of a partial wetting fluid spreading with $\theta_{eq} = 15°$ in figure 4-6 [19]. Differences in the volume are scaled out through the non-
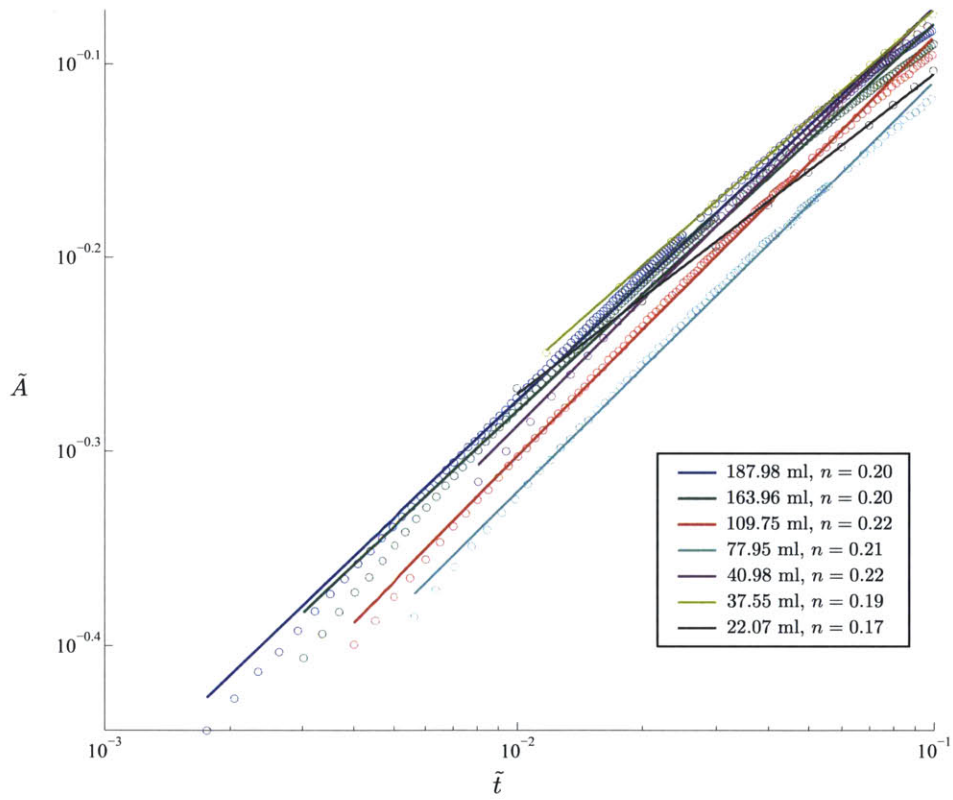
Figure 4-5: Nondimensionalized spread of various volumes of silicone oil in a partial wetting system, fitted with a power law relation of $\tilde{A} \sim \tilde{t}^n$. Lines represent the fit for a given volume, while ∘ represent the collected experiment data.

dimensionalization of the data. We use an initial condition with a small area, and another initial condition with a larger area. For the smaller area initial condition, we observe a power law corresponding to $A \sim t^{0.245}$ at early times, followed by a relaxation to the equilibrium configuration. The early spreading law closely matches with the scaling law given in equation 2.6, suggesting the early time experiences a gravity dominated spreading regime. For the initial condition with a larger starting area, we do not observe this gravity dominated regime, highlighting the impact of the intial condition on the appearance of a gravity dominated regime of flow.

In light of this dependence on initial area, we re-examine the early spreading behavior of the experimental data shown in figure 4-5. We choose the four experiments that start at the earliest times, and fit a power law to the first fifty data points in figure 4-7, finding an average $n = 0.23 \pm 0.01$. This is closer to the scaling for a gravity dominated regime described in equation 2.6, but the initial area is too close to the equilibrium area for the gravity dominated regime to appear.
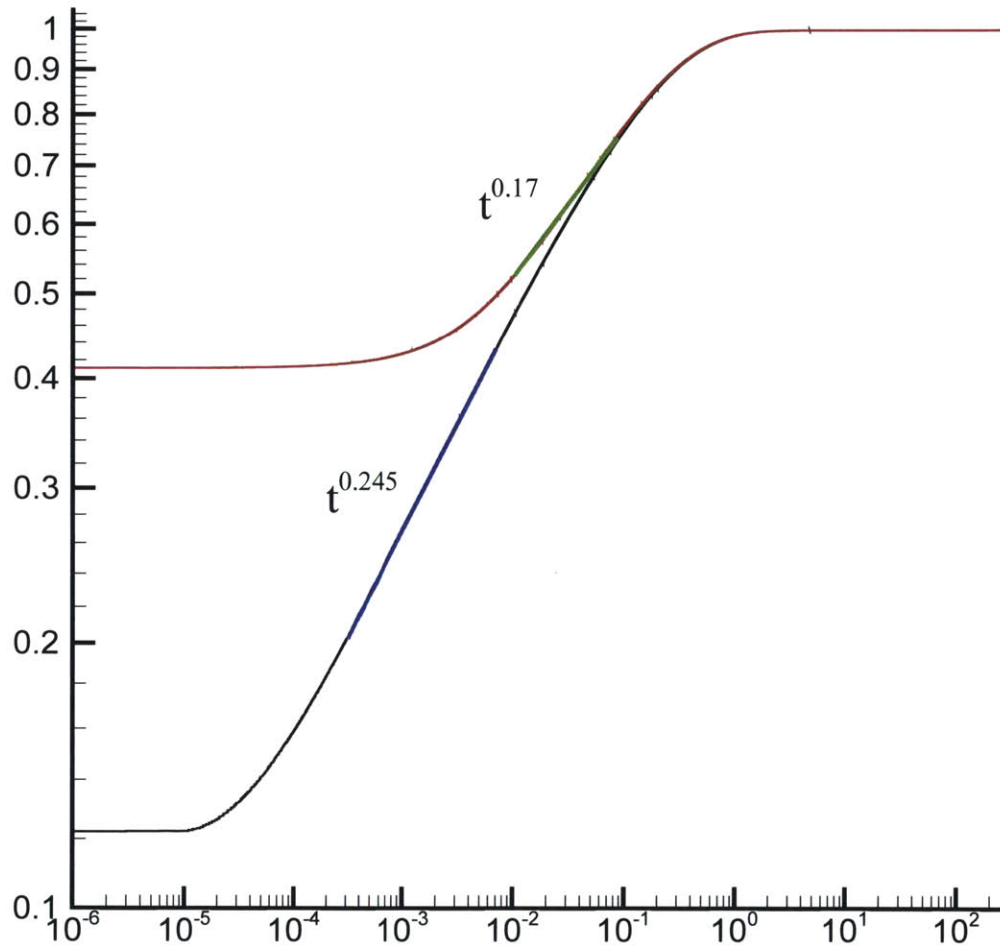
Figure 4-6: Nondimensionalized model of 7 mL of partial wetting fluid spreading on a flat, homogenous surface, using equation 2.13 [19]. There are two initial conditions, one for a small initial area, and one with a larger one. The smaller initial area results in the appearance a gravity dominated spreading regime of $\tilde{A} \sim \tilde{t}^{\frac{1}{4}}$.

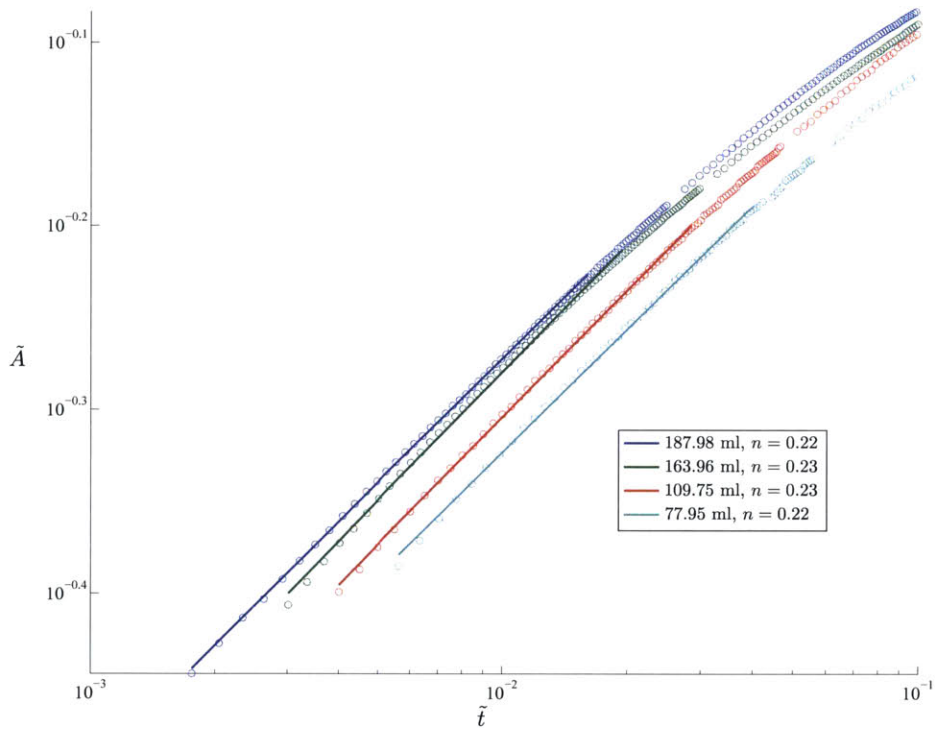Figure 4-7: Nondimensionalized spread of various volumes of silicone oil in a partial wetting system fitted with power laws of the form $\tilde{A} \sim \tilde{t}^n$. The solid lines represent polynomial fits for the first fifty data points, and $\circ$ represents the experimental data. The values for n are larger than seen in figure 4-5, but still do not match the scaling given by equation 2.6.

Chapter 5

Conclusions and Future Work

We have collected data on the spread of large volumes of fluid in a partial wetting system. As noted in section 2.2, there is a lack of experimental data covering this particular regime of fluid spreading, despite its common occurance, and this data begins to fill in this gap of knowledge. We see fairly uniform behavior when using the area and time scalings proposed in section 2.2, suggesting the only important parameter for partial wetting spread is the equilibrium contact angle, θ_{eq}. We observe an early regime of spreading, followed by a relaxation to a steady state. Predictions of the static fluid pancake height given by equation 2.7 closely match the measured and calculated heights found in section 3.1. Comparison with previously collected data on complete wetting also show similar early time behavior. Closer analysis of the early time spreading, however, reveals a difference in the complete and partial wetting. The complete wetting data closely matches the scaling predicted in section 2.1. However a theoretical explanation for the partial wetting data remains elusive, as seen in section 4.1.

In comparison to modeling results, we find both the model and experiments show a relaxation to the steady state. The model also appears to reveal an early time spreading regime corresponding to the gravity dominated spread derived in 2.1, depending on the intial area. The experimental data, however, did not cover the time periods when this regime occurs because the initial area was too large relative to the equilibrium area. Despite differences between the contact angle of the model and

37

experiments, there is similar behavior resulting from the partial wetting condition.

The differences between the model and the experiments highlight a few areas of future work. First, an expanded data set with a smaller initial area, ideally $\tilde{A}_i = 0.1$, is requried to examine the presence of a early spreading regime as predicted by the model. Second is a series of experiments using a variety of contact angles to verify the model results and develop understanding of the spreading dependence on the contact angle. Once the model is verified, the framework could then be expanded to account for multiphase flow in porous media, or other complex multiphase flow systems. The spread of a partially wetting fluid is a fundamental multiphase system. Understanding the flow in this situation will have important implications for other more complex multiphase problems.

Bibliography

[1] James Bird, Shreyas Mandre, and Howard Stone. Short-time dynamics of partial wetting. *Physical Review Letters*, 100(23):234501, 2008.

[2] Daniel Bonn, Jens Eggers, Joseph Indekeu, Jacques Meunier, and Etienne Rolley. Wetting and spreading. *Reviews of Modern Physics*, 81(2):739–805, 2009.

[3] John W. Cahn and John E. Hilliard. Free energy of a nonuniform system. I. Interfacial free energy. *The Journal of Chemical Physics*, 28(2):258, 1958.

[4] A. M. Cazabat and M. A. Cohen Stuart. Dynamics of wetting: effects of surface roughness. *The Journal of Physical Chemistry*, 90(22):5845–5849, 1986.

[5] R. Craster and O. Matar. Dynamics and stability of thin liquid films. *Reviews of Modern Physics*, 81(3):1131–1198, 2009.

[6] Luis Cueto-Felgueroso and Ruben Juanes. Macroscopic phase-field model of partial wetting: bubbles in a capillary tube. *Physical Review Letters*, 108(14):144502, 2012.

[7] Pierre-Gilles de Gennes. Wetting: statics and dynamics. *Reviews of Modern Physics*, 57(3):827–863, July 1985.

[8] Pierre-Gilles de Gennes, Françoise Brochard-Wyart, and David Quéré. *Capillarity and Wetting Phenomena*. Springer New York, New York, NY, 2004.

[9] E B Dussan. On the Spreading of Liquids on Solid Surfaces: Static and Dynamic Contact Lines. *Annual Review of Fluid Mechanics*, 11(1):371–400, 1979.

[10] Peter Ehrhard. Experiments on isothermal and non-isothermal spreading. *Journal of Fluid Mechanics*, 257(1):463, 1993.

[11] Peter Ehrhard and Stephen H. Davis. Non-isothermal spreading of liquid drops on horizontal plates. *Journal of Fluid Mechanics*, 229(1):365, 1991.

[12] S. Herminghaus. Universal phase diagram for wetting on mesoscale roughness. *Physical Review Letters*, 109(23):236102, 2012.

[13] H.E. Huppert. The propagation of two-dimensional and axisymmetric viscous gravity currents over a rigid horizontal surface. *Journal of Fluid Mechanics*, 121:43–58, 1982.

[14] Andrzej Latka, Ariana Strandburg-Peshkin, Michelle M. Driscoll, Cacey S. Stevens, and Sidney R. Nagel. Creation of prompt and thin-sheet splashing by varying surface roughness or increasing air pressure. *Physical Review Letters*, 109(5):054501, 2012.

[15] Becky Lavi and Abraham Marmur. The exponential power law: partial wetting kinetics and dynamic contact angles. *Colloids and Surfaces A: Physicochemical and Engineering Aspects*, 250(1-3):409–414, 2004.

[16] Marc Lebeau and Jean-Marie Konrad. A new capillary and thin film flow model for predicting the hydraulic conductivity of unsaturated porous media. *Water Resources Research*, 46(W12554), 2010.

[17] B. M. Marino, L.P. Thomas, J. A. Diez, and R. Gratton. Capillarity effects on viscous gravity spreadings of wetting liquids. *Journal of Colloid and Interface Science*, 30(3):14–30, 1996.

[18] Alexander Oron, Stephen H. Davis, and S. George Bankoff. Long-scale evolution of thin liquid films. *Reviews of Modern Physics*, 69(3):931–980, 1997.

[19] Amir A. Pahlavan. Doctoral dissertation, MIT, 2017. In progress.

[20] M. N. Popescu, G. Oshanin, S. Dietrich, and A. M. Cazabat. Precursor films in wetting phenomena. *Journal of Physics-Condensed Matter*, 24(24):243102, 2012.

[21] C. Redon, F. Brochard-Wyart, H. Hervet, and F. Rondelez. Spreading of "heavy" droplets. *Journal of Colloid and Interface Science*, 149(2):580–591, 1992.

[22] Weiqing Ren and Weinan E. Boundary conditions for the moving contact line problem. *Physics of Fluids*, 19(2):022101, 2007.

[23] L.H. Tanner. The spreading of silicone oil drops on horizontal surfaces. *Journal of Physics D: Applied Physics*, 12(9):1473–1484, 1979.

[24] Anish Tuteja, Wonjae Choi, Minglin Ma, Joseph M. Mabry, Sarah A. Mazzella, Gregory C. Rutledge, Gareth H. McKinley, and Robert E. Cohen. Designing superoleophobic surfaces. *Science*, 318(5856):1618–1622, 2007.

[25] T. Young. An essay on the cohesion of fluids. *Philosophical Transactions of the Royal Society of London*, 95:65–87, 1805.